Received: 6 October 2018 | Revised: 22 January 2019 | Accepted: 10 February 2019

DOI: 10.1111/gbb.12560

Genes, Brain and Behavior

ORIGINAL ARTICLE

Gene expression in the social behavior network of the wire-tailed manakin (*Pipra filicauda*) brain

Brent M. Horton[1] | **Thomas B. Ryder**[2] | **Ignacio T. Moore**[3] | **Christopher N. Balakrishnan**[4]

[1]Department of Biology, Millersville University, Millersville, Pennsylvania

[2]Migratory Bird Center, Smithsonian Conservation Biology Institute, Front Royal, Virginia

[3]Department of Biological Sciences, Virginia Tech, Blacksburg, Virginia

[4]Department of Biology, East Carolina University, Greenville, North Carolina

Correspondence
Christopher N. Balakrishnan, Department of Biology, East Carolina University, Howell Science Complex, Greenville, NC 27858.
Email: balakrishnanc@ecu.edu

Funding information
Division of Environmental Biology, Grant/Award Number: 1457541; Division of Integrative Organismal Systems, Grant/Award Number: 1353093; National Science Foundation, Grant/Award Numbers: 1456612, 1353085

The vertebrate basal forebrain and midbrain contain a set of interconnected nuclei that control social behavior. Conserved anatomical structures and functions of these nuclei have now been documented among fish, amphibians, reptiles, birds and mammals, and these brain regions have come to be known as the vertebrate social behavior network (SBN). While it is known that nuclei (nodes) of the SBN are rich in steroid and neuropeptide activity linked to behavior, simultaneous variation in the expression of neuroendocrine genes among several SBN nuclei has not yet been described in detail. In this study, we use RNA-seq to profile gene expression across seven brain regions representing five nodes of the vertebrate SBN in a passerine bird, the wire-tailed manakin *Pipra filicauda*. Using weighted gene co-expression network analysis, we reconstructed sets of coregulated genes, showing striking patterns of variation in neuroendocrine gene expression across the SBN. We describe regional variation in gene networks comprising a broad set of hormone receptors, neuropeptides, steroidogenic enzymes, catecholamines and other neuroendocrine signaling molecules. Our findings show heterogeneous patterns of brain gene expression across nodes of the avian SBN and provide a foundation for future analyses of how the regulation of gene networks may mediate social behavior. These results highlight the importance of region-specific sampling in studies of the mechanisms of behavior.

KEYWORDS

dominance, genome, songbird, systems biology, territoriality

1 | INTRODUCTION

Over the last two decades, our understanding of the neuroendocrine and genetic bases of vertebrate social behavior has progressed rapidly due to integrated studies of how hormones and gene expression interact to modulate brain function and, ultimately, behavior.[1,2] Much of this research has focused on well-defined neural circuits that are highly conserved across vertebrate taxa, such as the social behavior network (SBN) and the mesolimbic reward system (MRS), which together play complementary and integrated roles in regulating vertebrate social behavior.[3] The vertebrate SBN comprises six reciprocally connected brain regions, or nodes, located in the basal (ie, "limbic") forebrain and midbrain.[3,4] In mammals, these nodes are: (a) the extended medial amygdala, including the medial amygdala (MeA) and bed nucleus of the stria terminalis (BSTm), (b) the lateral septum (LS), (c) the preoptic area (POA), (d) the anterior hypothalamus (AH); (e) the ventromedial hypothalamus (VMH) and (f) the periaqueductal gray (PAG), including the intercollicular nucleus (ICo). Mounting evidence from multiple vertebrate taxa suggests that these SBN nodes are activated to varying degrees during social interactions and that collective neural activity across these nodes plays a key role in regulating various forms of social behavior (eg, sexual behavior, aggression, parental care and social affiliation).[3–7] The MRS is a predominantly dopaminergic neural circuit integral in evaluating the salience of external stimuli[8,9] and reinforcing behavioral responses to appropriate stimuli.[10,11] The MRS includes eight interconnected nuclei of the telencephalon and midbrain. In mammals, these nuclei are: (a) LS, (b) extended medial amygdala (MeA and BSTm), (c) basolateral amygdala, (d) hippocampus, (e) nucleus

accumbens; (f) ventral pallidum; (g) ventral tegmental area and (h) striatum. The SBN and MRS share two nodes (LS and extended MeA) and exhibit bidirectional connections between several brain regions. Indeed, the complementary functions of the SBN and MRS, and the linkage between them, support considering these circuits as an integrated neural system that governs social behavior.[3] Thus, the brain regions that comprise these networks are prime focal points for investigating how changes in neuroendocrine activity and gene expression modulate intraspecific and interspecific variation in behavior.[12–14]

The sex steroids and nonapeptide hormones (eg, vasopressin, oxytocin) are especially potent regulators of vertebrate social behavior. Accordingly, the brain regions of the SBN are generally rich in sex steroid and nonapeptide receptors and thus responsive to these hormones.[4,5,7,15–18] The sex steroids and nonapeptides can have multiple receptors,[19–22] and the distribution of these receptors determines the sensitivity of the SBN nodes to hormone action. In addition, regions of the SBN are, to varying degrees, sites of steroid and nonapeptide hormone synthesis and metabolism.[18,23] Our understanding of how these hormones act to modulate social behavior requires a holistic approach that can quantify the patterns of neuroendocrine gene expression that dictate hormone action in the SBN, including genes for hormone receptors, steroidogenic enzymes and nonapeptides. Moreover, steroids can act through both genomic and nongenomic pathways to affect gene expression and subsequent behavior.[19–21,24] As such, identifying the molecular products of steroid actions that influence neuron activity in the SBN can shed much needed light on the mechanistic underpinnings of steroid-mediated behavior.

The accessibility of RNA sequencing (RNA-seq) technology to researchers studying nontraditional model organisms provides new and exciting opportunities to deepen our understanding of the molecular pathways through which hormones influence the brain and behavior.[13,25–28] Functional genomics provides an ideal tool for beginning to understand how suites or networks of coexpressed genes modulate behavior. To date, a number of studies have leveraged whole-brain transcriptomic data to identify the gene expression profiles associated with sex, social status, ecotype and reproductive strategy within species,[26,28–30] as well as interspecific differences in reproductive and social behaviors across species.[31–33] Mounting evidence suggests, however, that patterns of gene expression vary among subdivisions of the vertebrate brain.[34–37] For example, studies of birds and mammals have showed distinctive gene expression profiles in the amygdala and hypothalamus,[38–40] suggesting that suites of behaviorally relevant genes are differentially expressed among nodes of the SBN. Indeed, results from candidate gene studies have showed that expression levels of key neuroendocrine genes can vary widely across regions of the SBN and that relationships between neuroendocrine gene expression and behavior are region-dependent.[18,40–42] Moving forward, it is therefore necessary to examine individual nuclei (or cell groups) as opposed to whole brains to learn how patterns of gene regulation across nodes of behavioral circuits shape variation in social behavior.[13] To our knowledge, no study has yet used whole-transcriptome sequencing to compare gene expression profiles across several nuclei of the avian SBN, the primary focus of this study.

To continue probing the neuroendocrine and genomic architecture of complex social behaviors, we used RNA-seq and weighted gene coexpression network analyses (WGCNAs) to describe region-specific patterns of gene expression across multiple nodes of the SBN and MRS in the male wire-tailed manakin (*Pipra filicauda*). As a group, the manakins (family Pipridae) are an emerging natural model system for comparative studies of complex social behavior and sexual selection due to the elaborate and diverse courtship displays and plumages exhibited by males across this clade. The wire-tailed manakin, in particular, provides a unique opportunity to examine the proximate and ultimate mechanisms underlying cooperative behavior. This Amazonian lek-breeding bird exhibits a rare form of male-male cooperation, whereby males form coalitions to perform cooperative courtship displays. Indeed, these males establish long-term display partnerships that form the basis of complex social networks, and which have clear fitness benefits for both territorial (ie, increased reproductive success)[43] and nonterritorial males (ie, increased probability of territory acquisition).[44] Territorial and nonterritorial males show substantial variation in behavioral phenotype, yet the hormonal and genetic bases for the differences in social behavior remain largely unknown. A prior study did show that circulating testosterone levels vary according to social status in male wire-tailed manakins,[45] indicating the steroid signaling pathways may play an important role in mediating male-male cooperation. For this reason, we focused here on gene expression across nodes of the SBN and regions of the MRS that are targets for sex steroids.

In the present study, we sequenced total RNA extracted from seven distinct brain nuclei (nucleus taenia, BSTm, LS, POM, VMH, ICo and arcopallium intermedium [AI]) representing five of the six nodes of the SBN, including the two nodes shared with the MRS. Nucleus taenia (TnA) is the proposed avian homolog of the mammalian MeA,[46] whereas the dorsomedial ICo and midbrain central gray (GCT) together comprise the avian homolog of the mammalian PAG.[47] We included the AI, a region putatively homologous to the mammalian ventral pallial amygdala,[48] in this analysis to represent an additional node of the MRS, and because this region is hypothesized to be involved in androgen-dependent display behavior in manakins.[49] We compared gene expression profiles among these seven regions to define patterns of uniqueness and congruity in gene expression across the SBN and MRS. In addition, we use WGCNA to describe gene networks and identify hub genes. Finally, we considered region-specific expression levels of candidate neuroendocrine genes involved in steroid and neuropeptide signaling to build a foundation for future studies of how hormone-signaling pathways modulate variation in male behavioral phenotype in this and other cooperative species. Because male testosterone levels vary according to social status in wire-tailed manakins,[45] we pay special attention to those genes involved in androgen signaling (eg, sex steroid receptors and steroidogenic enzymes) as well as those involved in the steroid-sensitive neuropeptide systems (eg, vasotocin, vasoactive intestinal peptide, and their receptors).

2 | METHODS

2.1 | Subjects and field sampling

We collected tissues from four male wire-tailed manakins (*Pipra filicauda*) near the Tiputini Biodiversity Station (0°38' S, 76°08' W) in the

Orellana province of eastern Ecuador during late December 2015, a period that coincides with peak breeding activity in this population. Males in this species can be categorized into four social classes according to plumage (age) and social status (territorial vs floater), as described by Ryder et al[43,45] The males we sampled represented two of these classes; two individuals were definitive plumage (ie, ≥third year) males that held display territories on leks, and two individuals were predefinitive plumage (ie, second year) males known as "floaters" because they did not hold display territories. Owing to small sample size we did not formally compare gene expression in males based on social status or age.

The birds were captured in mist nets on leks between 07:30 and 10:00, and blood sampled before being transported to a nearby workstation where they were euthanized via decapitation. Collection of birds was performed in accordance with Smithsonian ACUC #14-25 & 17-11. Whole brains were then extracted from the skull and rapidly frozen in powdered dry ice 4-6 minutes after euthanasia. Brains were kept frozen on dry ice for 1-4 hours in the field until they were transferred to a liquid nitrogen dry shipper (ThermoScientific, Waltham, Massachusetts) where they were stored at cryogenic temperatures for 14 to 16 days until imported into the United States. Once in the United States, brains were stored at −80°C for 6.5 months until cryosectioning, microdissection and RNA extraction (described below).

2.2 | Cryosectioning, microdissection and RNA extraction

Brains were cryosectioned at −12 to −14°C in the coronal plane consistent with the orientation used by Stokes et al. [50] Frozen sections 150 μm thick were briefly (<10 seconds) thaw-mounted onto Fisherbrand Premium Superfrost microscope slides, after which they were held on dry ice until microdissection. During microdissection, slides with adhered sections were placed on slabs (15 × 15 × 3 cm) of polished granite, which were kept frozen on dry ice throughout the procedure. With the aid of a stereomicroscope and fiber optic light source, seven brain regions of interest (ROIs) were located using readily identifiable landmarks (eg, fiber tracts, ventricles) and sampled by using a frozen, stainless steel tissue corer (Fine Science Tools, Foster City, California) to collect a 0.35, 0.50 or 0.80 mm diameter punch from the ROI. The punch diameter depended on the size of the ROI (see below).

We sampled the AI, as delineated by Fusani et al.,[49] by taking 0.8 mm punches from the left and right hemispheres of two consecutive sections. Nucleus taenia (TnA), as defined by Stokes et al,[50] and the medial bed nucleus of the stria terminalis (BSTm), as described by Kelly et al,[51] were sampled by taking 0.5 mm punches from the left and right hemispheres of four consecutive sections. The portion of the ICo medial to the nucleus mesencephalicus lateralis, pars dorsalis (MLd),[47,50] was sampled by taking 0.5 mm punches from the left and right hemispheres from four consecutive sections. We sampled the LS, as delineated by Goodson et al,[52] by taking 0.35 mm sections from the left and right hemispheres in four consecutive sections. Because the VMH[53] and medial preoptic area (POM)[54] are located at the midline of the brain, they were sampled by taking 0.8 mm punches centered on the midline to simultaneously capture the left and right portions of these ROIs; each ROI was sampled in three to four consecutive sections. Although we also sampled the AH and central mesencephalic gray (GCt), RNA yields from some samples of these regions were insufficient for sequencing and are not described hereafter.

Frozen tissue punches were placed directly into room temperature QIAzol lysis reagent (Qiagen, Hilden, Germany) and disrupted while thawing using a pellet pestle mixer and hand-held motor (Fisher Scientific, Hampton, New Hampshire). This lysate was then frozen at −80°C until the cryosectioning and microdissection of all brains were completed (≤3 days). The frozen tissue lysate was thawed and immediately passed through a QIAshredder spin column (Qiagen) to further homogenize tissue lysates. We then proceeded immediately with RNA extraction and purification, which was performed using miRNeasy Micro Kits (Qiagen) according to the manufacturer's recommended protocol for tissue samples containing <1 μg of RNA. We included an on-column DNase I digestion step using an RNase-Free DNase Set (Qiagen) according to the manufacturer's protocol for tissue samples containing <1 μg of RNA. Purified RNA was eluted with 14 μL of RNase-free water and stored at −80°C until quantitation and RNA integrity analysis. RNA extraction and purification for all samples was completed in a single run. Aliquots (1 μL) of purified RNA samples were quantitated using a Qubit fluorometer and a Qubit RNA HS Assay Kit (Invitrogen, Carlsbad, California). Total RNA concentrations ranged from 7.3 to 440.0 μg/mL (mean = 15.4 μg/mL). We assessed RNA integrity using the Agilent 2100 Bioanalyzer System and RNA 6000 Pico Kits (Agilent Technologies, Santa Clara, California). RNA integrity numbers (RINs) ranged 7.8 to 9.8 (mean = 8.95); RIN values were ≥ 8.0 for all but one sample.

2.3 | RNA-seq and analysis

Library preparation and sequencing were performed at the University of Illinois Roy J Carver Biotechnology Center. Thirty RNA-seq libraries were prepared using the TruSeq Stranded mRNAseq Sample Prep Kit; Illumina, San Diego, California. Libraries were quantitated by quantitative polymerase chain reaction and then sequenced on two lanes of an Illumina HiSeq 4000. Fastq files were generated and demultiplexed with bcl2fastq (v2.17.1.14). Adapter and quality trimming was performed using TrimGalore![55] under default settings. We then mapped reads to the *Manacus vitellinus* reference genome (ASM171598v1) using HiSat.[56] Manakins of the *Manacus* and *Pipra* genera are relatively closely related within the Family Pipridae,[57] so we expected interspecific read mapping to work well between these two taxa. To quantify the abundance of transcripts, we counted the number of reads that mapped to NCBI-predicted genes for the *M. vitellinus* genome using HT-seq.[58] We normalized count data for analysis using the variance-stabilized transformation in DE-Seq2.[59,60] After normalizing read counts using DE-Seq2, we used the plotPCA function in DE-Seq2 and PCAexplorer[61] to visualize and describe overall expression profiles. Principal components analysis (PCA) used the top 500 genes in the data set based on variance (Figure 1).

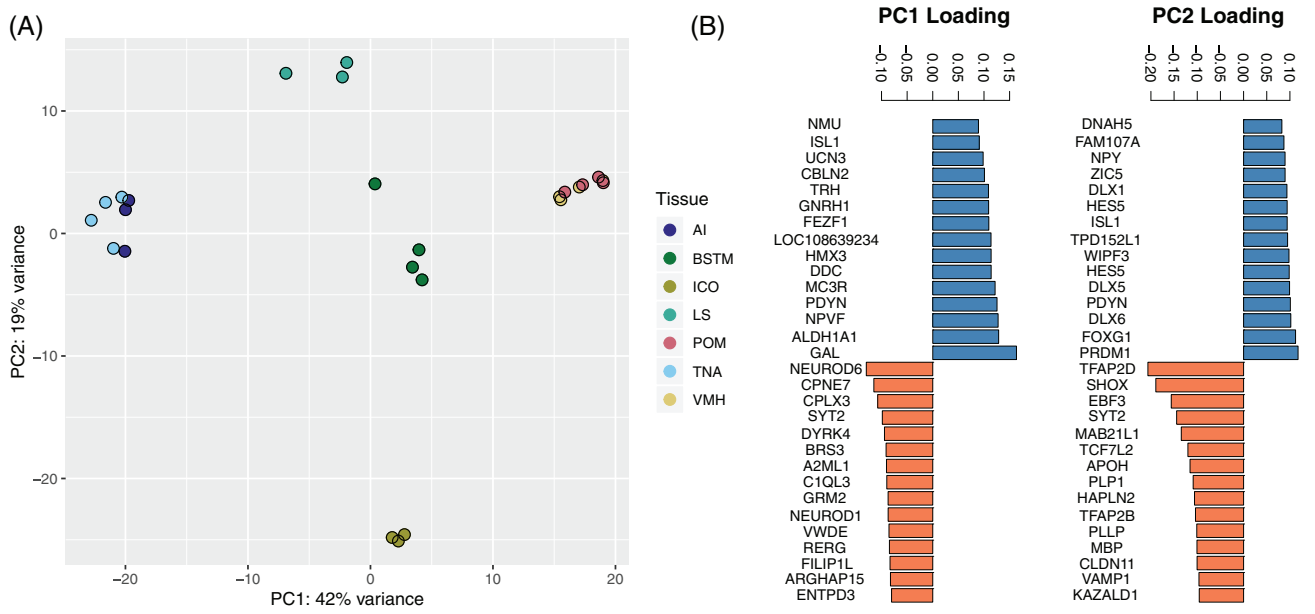

FIGURE 1 A, Scatterplot of principal component (PC) 1 vs PC2 reveals clustering of overall expression profile by brain region. B, Gene loadings (top 30) on each PC reveals regional differences in of neuropeptide (eg, GAL, PDYN) and developmental (DLX1, 5, 6) gene expression

2.4 | WGCNA and differential expression testing

We sought to identify networks of coregulated genes (genes with correlated expression patterns) that characterized each of the sampled nodes of the SBN. To this end, we used weighted-gene coexpression network analysis.[62,63] Unlike PCA, WGCNA does not impose orthogonality onto gene sets, and therefore is more appropriate for describing possible regulatory networks. Regulatory modules in WGCNA are created without *a priori* information on the sampling design. Using the variance stabilized count data from DE-Seq2, we generated a signed network by setting soft threshold power (β) = 18, minimum module size = 30, and module dissimilarity threshold = 0.30. Soft thresholding was chosen by plotting β against Mean Connectivity and selecting the point at which we observed a plateau in mean connectivity, representing a scale-free topology. Following module reconstruction we tested for correlations between modules and each of the seven sampled brain regions treating each as a binary variable (Figure 2). Because four individual birds were sampled, we also included the bird ID as a variable in the model.

We functionally characterized coexpression networks using gene ontology (GO) analysis using the rank-order based approach in GOrilla.[64] For each module, genes were ranked based on their module membership score determined in the WGCNA analysis. We preferred this rank-order based approach (as opposed to strict module assignment) as it reflects the correlation among modules, and because some genes could be assigned to multiple modules. GOrilla tests for enrichment towards the top of a gene list, where the "top" is defined based on the size of a particular GO category rather than an alpha value threshold. GOrilla also calculates an enrichment statistic based on N, the number of genes in the data set, B the number of genes in the whole dataset of a particular GO category, n, the number of genes in the top of the gene list and b, the number of genes that represent that GO category in the top of the gene list. Gene IDs were assigned based on annotation by NCBI and held in the gff file associated with the *Manacus* genome assembly. We then visualized the network structure for the top 500 strongest connections using a topological overlap measure and plotted the data in program R[65] using the iGraph[66] and ggnetwork packages. We identified module hubs as genes with more than 20 connections within this set.

All RNA-seq data have been deposited to GenBank (PRJNA437157). The raw count matrix and code for the WGCNA analysis are available at: https://github.com/chrisbalakrishnan/PipraFilicaudaRNAseq

3 | RESULTS

RNA-sequencing yielded an average of 26 million reads per sample. Seventy-two percent of the trimmed reads mapped to the genome and 49% of the reads could be unambiguously assigned to predicted transcripts using htseq-count. We detected expression (1 read in at least 1 individual) for 16 796 genes, or 89.5% of the 18 775 annotated genes in the genome. As required by WGCNA, we filtered low expression genes keeping 12 765 that passed WGCNA quality control criteria. Of these, 9598 could be linked to functional annotations in the GO database. Only these 9598 genes were used for GO analyses.

Principal components 1 and 2 explained 42.4% and 19.1% of the variation in the expression data, respectively (Figure 1A). Sample expression profiles clustered by the nucleus from which they were extracted (Figure 1A), reflecting consistency in dissection as well as brain region differences in gene expression. Gene expression profiles from the two hypothalamic nuclei, POM and VMH, were associated with positive PC1 values, whereas those from the amygdala (TnA) and the adjacent AI were associated with negative PC1 values. PC2 was also associated with brain region with high values for LS, intermediate values for POM, VMH, BSTm, AI and TnA, and low values for the

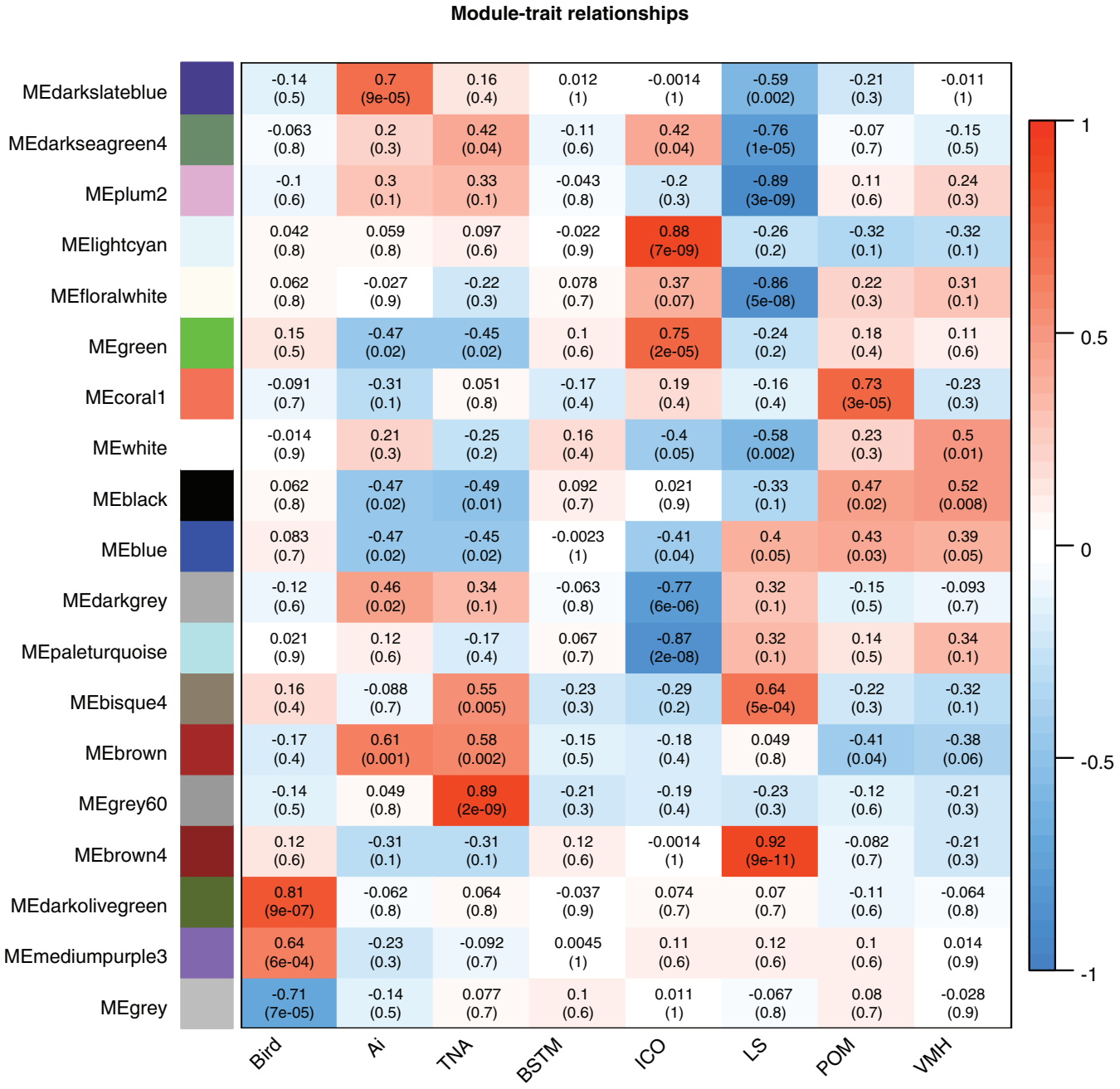

FIGURE 2 Statistical associations between expression profiles of each of the 19 reconstructed modules, individual brain regions and/or individual bird samples. Presented are correlation coefficients and associated *P*-values (within brackets). Note that the grey module is not a true module, but rather includes only those genes not assigned to other modules

midbrain nucleus ICo. Loadings for the genes most strongly associated with PC1 and 2 are presented in (Figure 1B). Many of the genes with strong, positive PC1 loadings are involved in neuropeptide signaling. These include galanin and GMAP prepropeptide (GAL), aldehyde dehydrogenase 1 family member A1 (ALDH1A1), neuropeptide VF precursor (NPVF), prodynorphin (PDYN) and melanocortin receptor 3R (MC3R). In contrast, genes with positive loadings on PC2 are involved with more developmental functions, including homeobox genes Distal-less homeobox (DLX1), DLX5, DLX6 and ISL Lim Homeobox 1 (ISL1). Neuropeptide Y (NPY) was also positively associated with PC2.

3.1 | Associations between expression networks and brain nuclei

Using the analysis parameters described previously, WGNCA analysis constructed a total of 19 modules (Figure 2). Sixteen modules showed expression patterns that were associated with at least one brain region in the SBN (see Figure 2). Based on our chosen module dissimilarity threshold, we retained some modules that showed similar expression patterns. For example, genes in the blue, black and white modules have relatively low expression in amygdala (TnA, AI) and high expression in hypothalamus (VMH, POM), whereas genes in the

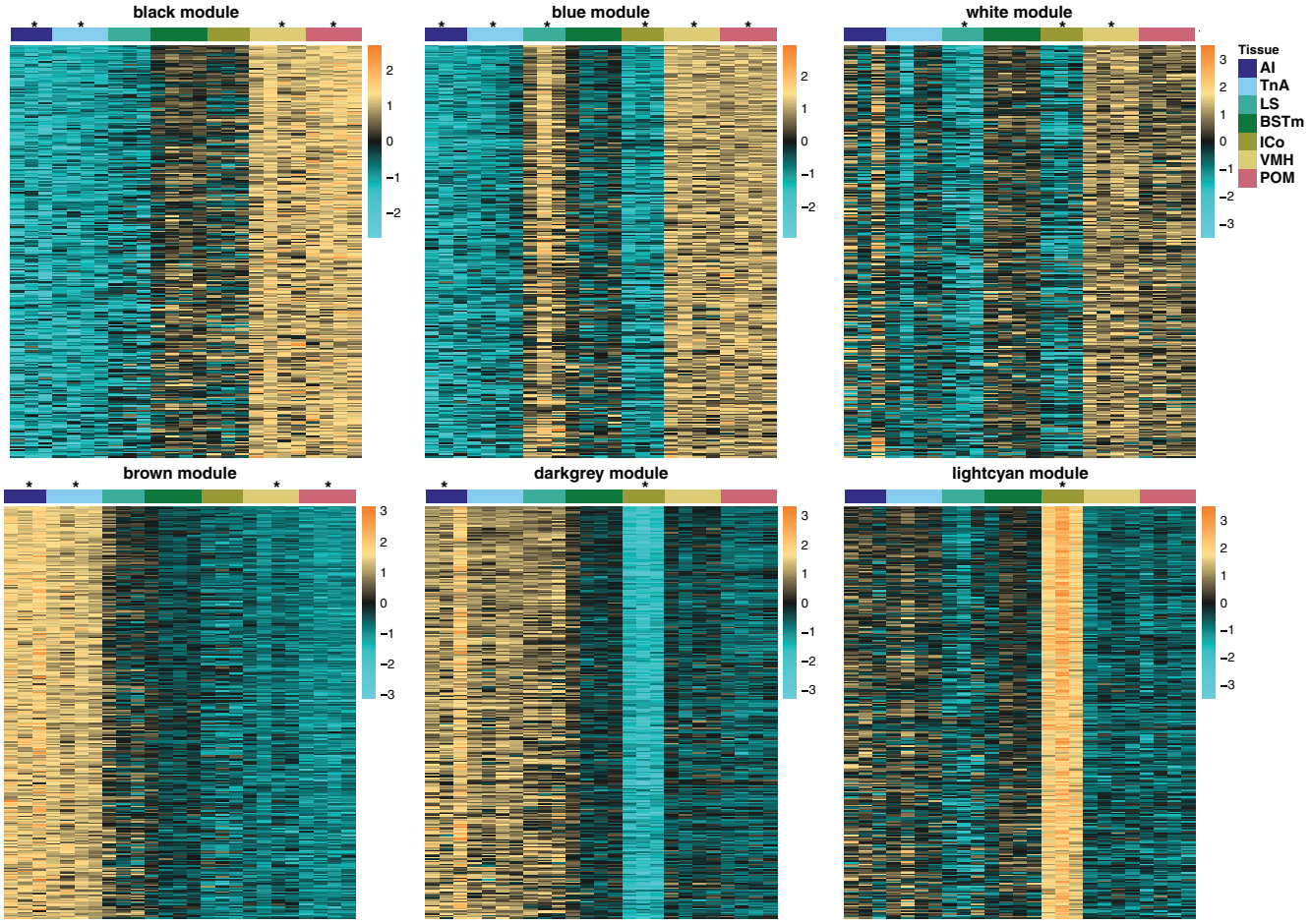

FIGURE 3 Heatmaps of top 300 genes associated with each of six modules (out of 19 total). Modules were selected for display based on their association with genes of interest (Table 1, Figure 4) and to highlight regional differences in gene expression. Asterisks indicate statistical associations ($P < 0.05$) between a module and brain region (see also Figure 2)

brown, dark gray and light cyan modules have the opposite expression pattern (Figure 3). Although more stringent merging of modules would have joined some of these modules, we retained these modules as distinct because they also reflect subtle and potentially important differences in regional patterns of gene coexpression (Figure 3). These differences were particularly apparent for genes with high module membership in their assigned module. For example, genes with high module membership in the black module (eg, progesterone receptor [PGR]) are distinguished from those assigned to the blue module (eg, proenkephalin [PENK]) by patterns of high and low expression in LS, respectively (Figure 4). Similarly, genes with high module membership in the brown module are differentiated from those assigned to the dark gray module by having low expression in LS. Module assignment for genes with lower module memberships, however, can be considered more ambiguous (despite statistical assignment to a particular module). An example of this is the gene for estrogen receptor alpha (ESR1), which was assigned to the blue module by WGCNA even though it has a higher estimated module membership for the black module (MMblue = 0.68 vs MMblack = 0.80, see Figure 4). Such patterns reflect the lack of orthogonality in WGCNA modules; that is, a given gene can be associated with multiple regulatory networks. As such, genes like ESR1 with similar module membership in multiple modules are ambiguous in module assignment. Three modules, including the "gray" module which comprises the set of unclustered genes (20 genes) showed significant variation among individual birds (mediumpurple3, $r = 0.64$, $P = 6e\text{-}04$; dark olive green, $r = 0.81$, $P = 9e\text{-}07$).

3.2 | Examination of neuroendocrine candidate genes

To highlight the relationship between WGCNA modules and genes related to neuroendocrine signaling and behavior, we compiled a list of genes encoding key hormones, steroidogenic enzymes, and hormone receptors (Table 1, Figure 4). In doing so we observed that the majority of the well-studied neuropeptides and hormone receptors (eg, vasoactive intestinal polypeptide [VIP], DRD1, ESR1, androgen receptor [AR]) were assigned to just four modules, blue, black, brown and dark gray, representing the two opposing gradients of expression described above. For example, AR (black module), ESR1 (blue module), PGR (black module) and VIP (black module) all show high expression in the hypothalamic nuclei (POM and VMH) and low expression in the amygdala (Table 1; Figure 4). By contrast, neuroendocrine genes in the brown module (eg, HTR6, DRD, CNR1) had low expression in those same hypothalamic nuclei but high expression in the amygdala (Figure 4). These four modules also included a number of serotonin

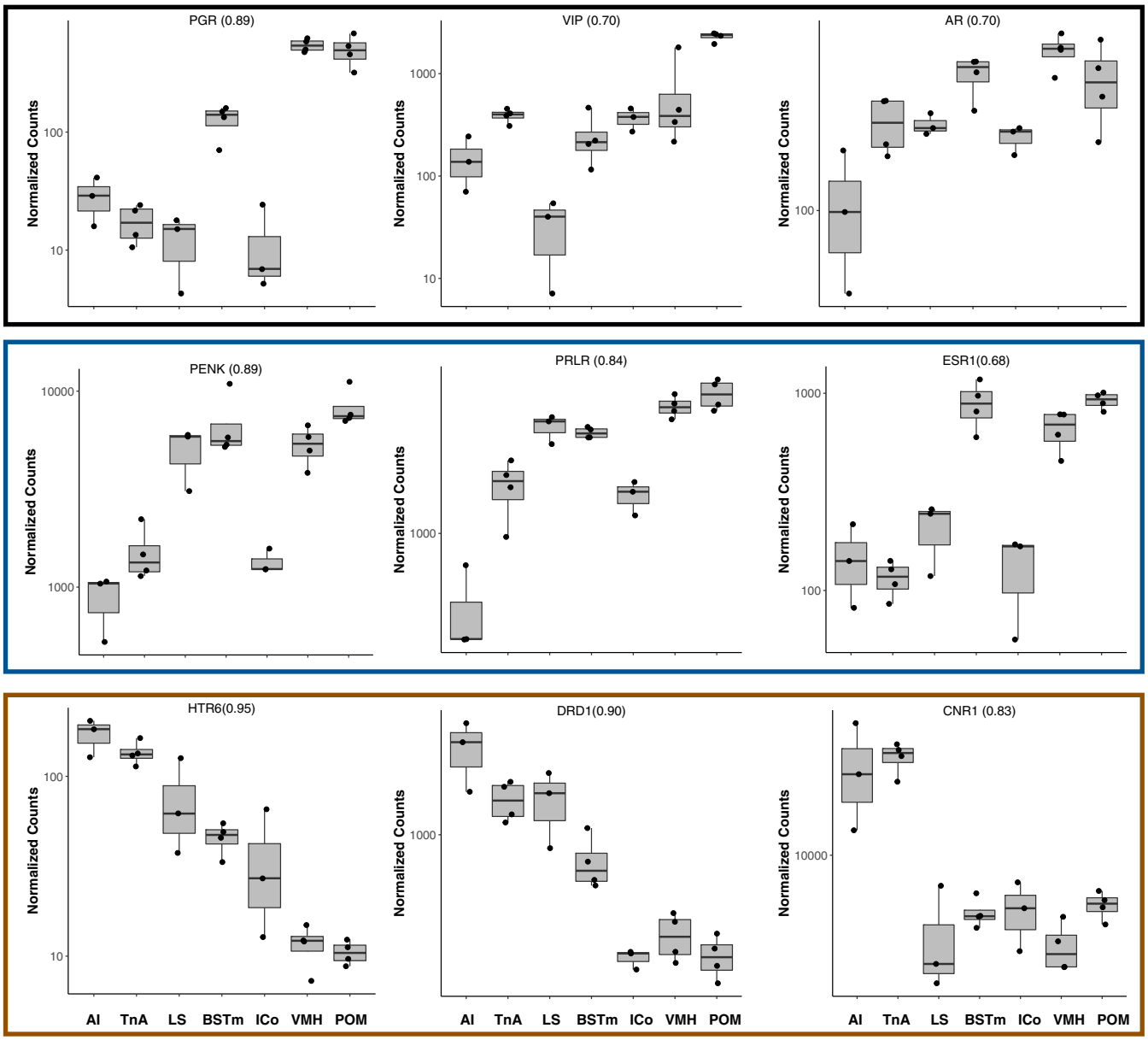

FIGURE 4 Expression plots (normalized read counts) for candidate genes associated with three key modules, blue, black and brown. Module assignment is denoted by the colored box around each panel of three genes. Module membership for each gene is presented within parentheses besides each gene name

and dopamine receptors, as well as insulin receptor and the cannabinoid receptor CNR1 (Table 1).

Other candidate neuroendocrine genes were distributed among five other coexpression modules (Table 1). In general, these genes had lower module membership values (MM = 0.32-0.77), indicating lower specificity of expression among sampled brain regions. Among these are two genes involved in steroid metabolism, including 5-alpha reductase (SRD25A) and aromatase assigned to the light cyan (MM = 0.41) and white (MM = 0.77) modules, respectively. Two key nonapeptide hormone-encoding genes, OXT (encoding oxytocin and neurophysin1) and AVP (encoding arginine vasopressin, neurophysin 2 and copeptin) were not annotated in the *M. vitellinus* genome, and thus we do not have information on their expression. We focus the remainder of our analysis on the six modules within which candidate genes were most strongly represented (Figure 3).

Analysis of regional variation in gene expression across SBN regions also enables us to describe patterns among paralogous hormone receptors. Gene duplication and subsequent sub- or neofunctionalization provides a mechanism by which hormonal action can be modulated to have context and region-specific effects,[67,68] and thus has played an important role in the evolution of hormonal signaling.[69,70] We specifically examined paralogous receptor genes for estrogen, galanin, vasoactive intestinal peptide, serotonin, neuropeptide Y, dopamine, somatostatin and GABA (Table 1). All of these gene families except for the GABA receptors (R1, R3, B3) included members that that were assigned to different modules indicating some degree of expression divergence for each gene family.

TABLE 1 Module assignment for key hormones, receptors and enzymes

Module	Gene ID	Gene	Function	Module membership
Black	DDC	DOPA decarboxylase	Enzyme	0.98
	GAL	Galanin	Neuropeptide	0.91
	CYP1b1	Cytochrome p450 1b1	Enzyme	0.91
	TRHR	Thyrotropin-releasing hormone receptor	Receptor	0.90
	PGR	Progesterone receptor	Receptor	0.89
	MC3R	Melanocortin receptor 3R	Receptor	0.88
	TRH	Thyrotropin-releasing hormone	Hormone	0.81
	ESR2	Estrogen receptor 2	Receptor	0.81
	HTR1F	Serotonin receptor 1F	Receptor	0.80
	PDYN	Prodynorphin	Hormone	0.74
	GALR3	Galanin receptor 3	Receptor	0.72
	CALCB	Calcitonin-related polypeptide beta	Neuropeptide	0.72
	GNRH1	Gonadotropin-releasing hormone 1	Hormone	0.70
	AR	Androgen receptor	Receptor	0.70
	VIP	Vasoactive intestinal polypeptide	Neuropeptide	0.70
	NPVF	Neuropeptide VF precursor	Neuropeptide	0.70
	TAC1	Tachykinin	Neuropeptide	0.58
	POMC	Pro-opiomelanocortin	Neuropeptide	0.54
	PRLHR	Prolactin-releasing hormone receptor	Receptor	0.47
Blue	GALR1	Galanin receptor 1	Receptor	0.89
	PENK	Proenkephalin	Neuropeptide	0.86
	PRLR	Prolactin receptor	Receptor	0.84
	ESR1	Estrogen receptor 1	Receptor	0.68
	HTR2B	Serotonin receptor 1B	Receptor	0.63
	VIPR1	VIP receptor 1	Receptor	0.62
	NPY5R	Neuropeptide receptor 5R	Receptor	0.60
	DRD2	Dopamine receptor D2	Receptor	0.46
	NTS	Neurotensin	Neuropeptide	0.38
	HTR2A	Serotonin receptor 2A	Receptor	0.37
Brown	HTR6	Serotonin receptor 6	Receptor	0.95
	DRD1	Dopamine receptor 1	Receptor	0.90
	CNR1	Cannabinoid receptor 1	Receptor	0.83
	HTR2C	Serotonin receptor 2C	Receptor	0.82
	DRD5	Dopamine receptor 5	Receptor	0.75
	SSTR4	Somatostatin receptor 4	Receptor	0.62
	HTR1B	Serotonin receptor 1B	Receptor	0.44
Darkgrey	VIPR2	VIP receptor 2	Receptor	0.86
	NPY1R	Neuropeptide receptor 1R	Receptor	0.82
	INSR	Insulin receptor	Receptor	0.78
	GABBR1	GABA receptor R1	Receptor	0.72
	GABRR3	GABA receptor R3	Receptor	0.67
	GABRB3	GABA receptor B3	Receptor	0.65
	NPY	Neuropeptide Y	Neuropeptide	0.58
	HTR7	Serotonin receptor 7	Receptor	0.55
Lightcyan	SST	Somatostatin	Hormone	0.64
	HTRA2	Serotonin receptor A2	Receptor	0.59
	SRD5A2	5 alpha reductase	Enzyme	0.41
White	CYP191A1	Aromatase	Enzyme	0.77
	NTSR1	Neurotensin receptor 1	Receptor	0.68
	SSTR3	Somatostatin receptor R3	Receptor	0.66
	SSTR1	Somatostatin receptor R1	Receptor	0.56
Brown4	DRD3	Dopamine receptor D3	Receptor	0.72
	HTR5A	Serotonin receptor 5A	Receptor	0.65
	AVT	Arg8-vasotocin receptor (VT1)	Receptor	0.32
Green	OXTR	Oxytocin receptor (VT3)	Receptor	0.37
	HTR1A	Serotonin receptor 1A	Receptor	0.73
Plum1	AVPR1A	Arginine vasopressin receptor 1A (VT4)	Receptor	0.79

3.3 | Functional annotation of WGCNA modules

In addition to the candidate gene approach, we used GO analysis to systematically characterize WGCNA modules in terms of function. These analyses showed two broad themes in terms of functional enrichment. As might be expect based on the candidate gene analysis, we observe enrichment for GO categories related to neuropeptide signaling and hormone receptor activity across multiple modules (Supporting information Tables S1-S6). As in the PCA presented above, we also observed an enrichment of terms related to developmental processes and tissue differentiation in the brain.

As the modules themselves have correlated expression patterns, GO analyses based on module memberships were similar. The white and black modules (high hypothalamic expression but low expression in the amygdala) showed significant enrichment for multiple GO categories related to neuropeptide signaling (eg, "neuropeptide signaling pathway", white: P = 3.22e-04, black: P = 0.04; "dopamine metabolic process", white, P = 0.04, Tables S1 and S2). The black module also showed an enrichment for genes involved in "developmental process" (P = 0.02) including the orthopedia homeobox gene (OTP, MM = 0.91). This module was also enriched for genes in the "smoothened pathway" (P = 0.02), including the classic developmental morphogen sonic hedgehog (SHH, MM = 0.80) and its receptors patched 1 (PTCH1, MM = 0.83) and PTCH2 (MM = 0.82). Although some of our candidate neuroendocrine-related genes mapped to the blue module (Table 1), this module was primarily enriched for GO categories related to development and regional differentiation (eg, "pattern specification" (P = 3.0E-11) and "determination left/right symmetry" (P = 6.5E-09), Table S2). The strongest enrichments in the blue module were a large set of categories related to cilium morphology, which may relate to aspects of cellular structure and compositional differences among brain regions.

Among the modules that had high expression in the amygdala (TnA) and AI, both the brown and dark gray modules (Tables S3 and S4) were significantly enriched for GO categories relating to synaptic transmission, plasticity (dark gray, P = 3.5e-06), and learning and memory (dark gray, P = 7.8e-04). These categories include dopamine receptors DRD1 and DRD5, cannabinoid receptor CNR1, and a suite of glutamate receptors (GRIN2A, GRIN2B, GRM2, GRIA2 and GRIA3). The dark gray module also included signatures of development-related genes, including those associated with "positive regulation of dendritic spine development" (P = 3.14e-04). Although the light cyan and dark gray modules had similar expression profiles in the hypothalamus and amygdala, genes expression patterns in the LS differed markedly between these modules, with low expression for light cyan genes but high expression for dark gray genes (Figure 3). Genes strongly associated with the light cyan module (Table S5) were highly enriched for functions related to cellular energetics (eg, "mitochondrial electron transport, NADH to ubiquinone" [P = 5.4e-12], "generation of precursor metabolites and energy", P = 6.5e-12).

Two modules with the strongest enrichment for behavior-related genes were the black and dark gray modules. Thus, we further examined the topology of these networks to better characterize potential regulatory interactions. In the black module, the most highly connected hub gene encodes the synaptic organizer protein CBLN2 (98 connections, Figure 5). Two other key hubs were serine/threonine kinase 32B (STK32B, 68 connections) and DOPA decarboxylase (DDC, 21 connections; Figure 5). DDC also had the highest module membership among genes in the black module. In the dark gray module, the gene with highest connectivity was Signal Induced Proliferation Associated 1 like 1(SIPA1L1, 95 connections among the top 500 genes). Additional highly connected genes in this module include a series of glutamate-related genes (GRIN2B, SHANK2, DLGAP1 and DLGAP2).

4 | DISCUSSION

We have provided here a fundamental picture of gene expression across several nodes of the vertebrate SBN. These heterogeneous patterns of gene expression reflect differences in both the neuronal activity and cellular composition among brain regions known to be integral in regulating social behavior. Overall, our results show opposing gradients of expression among gene modules, whereby some suites of genes are highly expressed in the hypothalamic nuclei and lowly expressed in the amygdala, or vice versa. Genes tightly associated with 19 defined regulatory modules show distinctive expression signatures that differentiate each of the sampled SBN and MRS nodes. Our finding that behaviorally relevant brain nuclei have distinctive gene co-expression patterns highlights the importance of nucleus-level resolution for understanding the neurogenomic bases of vertebrate social behavior. Moving forward, fine-scale approaches will be most successful in showing meaningful relationships between neural gene expression and behavior.

The majority of candidate loci encoding neuropeptide hormones, steroid and neuropeptide hormone receptors, and steroidogenic enzymes were associated with modules (ie, black, blue and white modules) that showed high hypothalamic expression and low amygdalar expression (ie, Figure 3). This finding underscores how high levels of neuropeptide activity and steroid sensitivity in some SBN brain regions play integral roles modulate vertebrate social behavior (eg, [5]). A subset of serotonin, dopamine and cannabinoid receptors associated with the brown module show the opposite pattern, with high expression in the nuclei shared by the SBN and MRS (TnA, LS) and a nucleus of the MRS (AI), but low expression in hypothalamic nuclei (POM, VMH). This pattern likely reflects functions of these genes and brain regions in reward circuitry.[71] The MeA (TnA) and pallial amygdala (AI) were also enriched for genes involved in synaptic plasticity, especially for genes associated with glutamate receptor activity (eg, GRIN2A, GRIN2B, FMR1, TRPM1, HOMER1, GRIA3, GRIA2, GRIN3A). Across the SBN, we observed striking variation in the distribution of various transmembrane receptors (eg, ion-channel genes), a pattern similar to that observed in an analysis of variation in gene expression across the song control system in songbirds.[35]

DDC was the gene with the highest module membership in the black module, where it was a highly interconnected hub gene (21 of the 500 strongest connections, Figure 5). DDC is an enzyme that catalyzes the production of dopamine and serotonin from their respective precursors, tyrosine and tryptophan. Indeed, the constructed network connected DDC with GTP cyclohydrolase 1 (GCH1), another enzyme

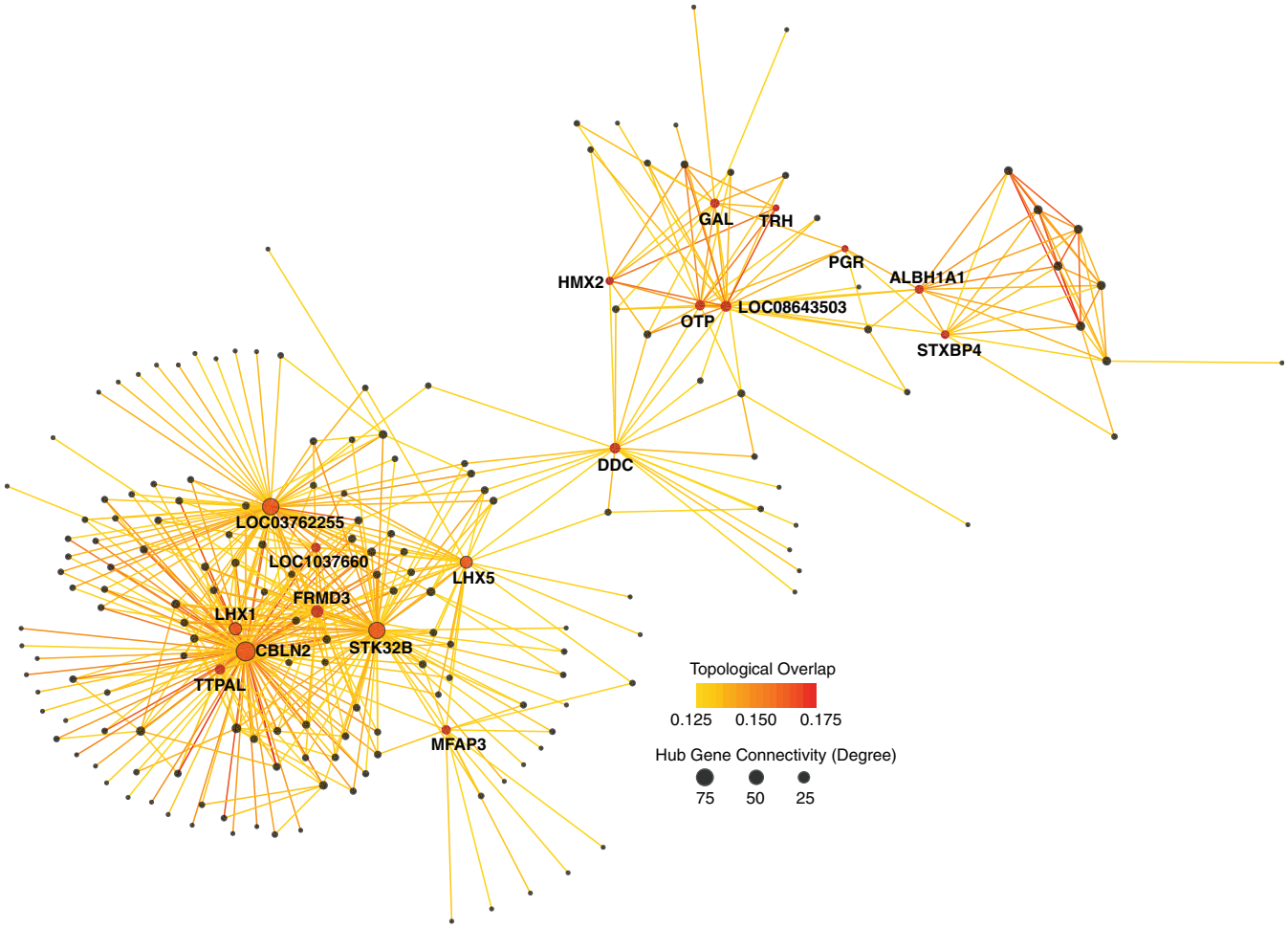

FIGURE 5 Network diagram of top 500 genes in the black module. Gene names are shown only for hub genes (>20 connections). DOPA decarboxylase (DDC) and orthopedia homeobox (OTP) link neuroendocrine genes (progesterone receptor [PGR], thyrotropin-releasing hormone [TRH]) with more developmental (LHX1, LHX5) subnetworks. Cerebellin 2 (CBLN2) is the most highly connected hub gene

involved in the production of dopamine and serotonin. As a module hub gene, DDC also linked the "neuro-endocrine" and "developmental" components of this regulatory network (Figure 5). On the neuroendocrine side, DDC has direct links to genes for PGR, thyrotropin-releasing hormone receptor (TRHR), galanin and galanin message-associated peptide (GAL), and a ghrelin receptor (GHSR). DDC, however, is also linked to genes with developmental functions like LIM Homeobox 5 (LHX5, also a hub, 29/500 strongest connections), SHH and OTP among others. The most highly interconnected gene within the black module was cerebellin2 (CBLN2), a gene with known roles in the structural organization of synapses.[72] SSH as well as other LIM homeobox genes (LHX6/7) have previously been described as markers of nodes within the MRS and/or SBN.[3]

The neuropeptide gene with the highest membership in any module was galanin (GAL, 14 connections, MMblack = 0.91; Figure 5, Table 1). Galanin and its receptors are known to be abundant in the hypothalamus and POA of the mammal brain,[73] where galanin actions may influence dopamine, oxytocin, and gonadotropin-releasing hormone (GnRH) release.[74] Galanin is also believed to play a role in the MRS.[75] Consistent with its known pleiotropy, GAL, like DDC, holds a key node in the black regulatory module (14 connections, MM = 0.98). GAL is directly linked to PGR, TRH, TRHR, GHSR, SSH and OTP in the black module. These connections between GAL, DDC and OTP are especially interesting because of the known role of OTP in neuronal differentiation. Both OTP and Nescient Helix-Loop-Helix 2 (NHLH2, also assigned to the black module, MM = 0.91) play a role in the specification of POMC (Pro-opiomelanocortin), NPY, agouti-related neuropeptide, GnRH and dopaminergic neurons within the hypothalamus.[76,77] Likewise, OTP and POU3F2 (POU Class 3 Homeobox 2, not annotated in our data set) are required for the expression of oxytocin, vasopressin, TRH and corticotropin-releasing hormone in hypothalamic neurons.[76] Thus, our reconstructed network supports known regulatory interactions between OTP and multiple neurohormones.

Most of the examined neuropeptide receptor gene families examined include paralogs that were assigned to different modules. This finding supports an evolutionary model of gene regulatory divergence following gene duplication. One exception to this rule was that all three detected GABA receptors were assigned to the same module (Table 1). Likewise, ESR1 and GALR3 were assigned to the black module, whereas ESR2 and GALR1 were assigned to the blue module. As mentioned previously, black and blue modules show parallel expression patterns so paralogous estrogen and galanin receptors do as well. By contrast, more striking differences in expression (ie, assignment to

modules with contrasting expression patterns) is observed for VIPR1 vs VIPR2 and NPY1R vs NPY2R and NPY3R. A particularly interesting case is the DRD1 and DRD2 dopamine receptors, which are assigned to brown and blue modules, respectively. DRD1 and DRD2 have independently evolved the ability to bind dopamine from serotonin receptors.[78] DRD1 is more closely related to the serotonin receptors 5HT4 and 5HT6, and shares a more similar expression pattern with these serotonin receptors than it does DRD2. DRD2, on the other hand, shares a more similar expression pattern to serotonin receptor 5HT2, to which it is more closely related. Comparative studies across species with varying gene complements could show the history of possible neo- and sub-functionalization of these genes.

One limitation of our study is that we had relatively small sample sizes within brain regions. Thus, patterns of regulatory network structure are driven primarily by expression differences among nuclei and assume a shared regulatory network architecture across regions. Larger sample sizes (~n = 20-30) would enable us to test for variation in network structure among regions. While the results presented here accurately define the expression profiles of the different brain regions, this approach falls short of identifying regional differences in network architecture that may exist.

Here, we contribute analyses and new evidence to a growing body of research showing the heterogeneity of gene expression in the vertebrate brain. By describing gene expression heterogeneity in functionally integrated nuclei within the vertebrate SBN (and MRS), our findings illustrate the importance of examining region-specific gene expression across multiple, behaviorally relevant nuclei to elucidate links between genes and behavior. Importantly, our work highlights the feasibility of detailed neurogenomic analyses in a nontraditional model system studied in a field setting. Moreover, we hope that our results will encourage similar approaches in future studies of the molecular mechanisms regulating complex social behavior in diverse taxa. Manakins, as an example, display an impressive diversity of social structures including elaborate cooperative behaviors among males. Viewed cumulatively, this study lays the foundation for future work on how variation in neural gene expression across nodes of the SBN may underlie differences in male social status and associated behavioral phenotypes.

ACKNOWLEDGMENTS

The authors thank David Clayton and Daniel Newhouse for providing feedback on drafts of this manuscript. Daniel Newhouse also provided assistance with code for WGCNA analyses. Ben Vernasco and Jennifer Houtz assisted with sample collection in the field. Matthew Fuxjager and Susan Fahrbach provided access to lab space and equipment at Wake Forest University, where cryosectioning, microdissection, and RNA extraction were carried out. Export and import permits included MAE-DNB-CM-2015-0008, 006-016-EXP-1C-FAU-DNB/MA & USDA APHIS 126133. The development of this work was facilitated by a NSF Research Coordination Network grant (1457541). Funding for this work was provided by NSF 1353085 (T.B.R., I.T.M. and B.M.H.) and 1456612 (C.N.B.).

Author Contributions

B.M.H. designed the study, conducted field and lab work and wrote the manuscript. T.B.R. designed the study, conducted field work, assisted with analyses and wrote the manuscript. I.T.M. designed the study, conducted field work and wrote the manuscript. C.N.B. designed the study, analyzed the RNA-seq data and wrote the manuscript.

ORCID

Brent M. Horton https://orcid.org/0000-0002-3355-1613
Thomas B. Ryder https://orcid.org/0000-0002-5517-6607
Ignacio T. Moore https://orcid.org/0000-0001-8875-8913
Christopher N. Balakrishnan https://orcid.org/0000-0002-0788-0659

REFERENCES

1. Ben-Shahar Y, Robichon A, Sokolowski MB, Robinson GE. Influence of gene action across different time scales on behavior. *Science*. 2002; 296:741-744.
2. Robinson GE, Fernald RD, Clayton DF. Genes and social behavior. *Science*. 2008;322:896-900.
3. O'Connell LA, Hofmann HA. Evolution of a vertebrate social decision-making network. *Science*. 2012;336:1154-1157.
4. Newman SW. The medial extended amygdala in male reproductive behavior. A node in the mammalian social behavior network. *Ann N Y Acad Sci*. 1999;877:242-257.
5. Goodson JL. The vertebrate social behavior network: evolutionary themes and variations. *Horm Behav*. 2005;48:11-22.
6. Goodson JL, Saldanha CJ, Hahn TP, Soma KK. Recent advances in behavioral neuroendocrinology: insights from studies on birds. *Horm Behav*. 2005;48:461-473.
7. O'Connell LA, Hofmann HA. The vertebrate mesolimbic reward system and social behavior network: a comparative synthesis. *J Comp Neurol*. 2011;519:3599-3639.
8. Deco G, Rolls ET. Attention, short-term memory, and action selection: a unifying theory. *Prog Neurobiol*. 2005;76:236-256.
9. Wickens JR, Budd CS, Hyland BI, Arbuthnott GW. Striatal contributions to reward and decision making: making sense of regional variations in a reiterated processing matrix. *Ann N Y Acad Sci*. 2007;1104: 192-212.
10. Numan M. Motivational systems and the neural circuitry of maternal behavior in the rat. *Dev Psychobiol*. 2007;49:12-21.
11. Fuxjager MJ, Forbes-Lorman RM, Coss DJ, Auger CJ, Auger AP, Marler CA. Winning territorial disputes selectively enhances androgen sensitivity in neural pathways related to motivation and social aggression. *Proc Natl Acad Sci U S A*. 2010;107:12393-12398.
12. O'Connell LA, Hofmann HA. Genes, hormones, and circuits: an integrative approach to study the evolution of social behavior. *Front Neuroendocrinol*. 2011;32:320-335.
13. Rubenstein DR, Hofmann HA. Proximate pathways underlying social behavior. *Curr Opin Behav Sci*. 2015;6:154-159.
14. Baran NM, McGrath PT, Streelman JT. Applying gene regulatory network logic to the evolution of social behavior. *Proc Natl Acad Sci U S A*. 2017;114:5886-5893.
15. Morrell JI, Pfaff DI. A neuroendocrine approach to brain function: localization of sex steroid concentrating cells in vertebrate brains. *Am Zool*. 1978;18:447-460.
16. McEwen BS. Steroid hormones and the brain: cellular mechanisms underlying neural and behavioral plasticity. *Psychoneuroendocrinology*. 1980;5:1-11.
17. Goodson JL, Bass AH. Social behavior functions and related anatomical characteristics of vasotocin/vasopressin systems in vertebrates. *Brain Res Brain Res Rev*. 2001;35:246-265.
18. Goodson JL, Kingsbury MA. Nonapeptides and the evolution of social group sizes in birds. *Front Neuroanat*. 2011;5:13.

19. Kohno S, Katsu Y, Iguchi T, Guillette LJ. Novel approaches for the study of vertebrate steroid hormone receptors. *Integr Comp Biol*. 2008;48:527-534.
20. Guerriero G. Vertebrate sex steroid receptors: evolution, ligands, and neurodistribution. *Ann N Y Acad Sci*. 2009;1163:154-168.
21. Hasunuma I et al. Roles of arginine vasotocin receptors in the brain and pituitary of submammalian vertebrates. *Int Rev Cell Mol Biol*. 2013; 304:191-225.
22. Klatt JD, Goodson JL. Oxytocin-like receptors mediate pair bonding in a socially monogamous songbird. *Proc Biol Sci*. 2013;280:20122396.
23. Balthazart J, Baillien M, Cornil CA, Ball GF. Preoptic aromatase modulates male sexual behavior: slow and fast mechanisms of action. *Physiol Behav*. 2004;83:247-270.
24. Rudolph LM, Cornil CA, Mittelman-Smith MA, et al. Actions of steroids: new neurotransmitters. *J Neurosci Off J Soc Neurosci*. 2016;36: 11449-11458.
25. Robinson GE, Banks JA, Padilla DK, et al. Empowering 21st century biology. *Bioscience*. 2010;60:923-930.
26. Cardoso SD, Teles MC, Oliveira RF. Neurogenomic mechanisms of social plasticity. *J Exp Biol*. 2015;218:140-149.
27. MacManes MD, Austin SH, Lang AS, Booth A, Farrar V, Calisi RM. Widespread patterns of sexually dimorphic gene expression in an avian hypothalamic-pituitary-gonadal (HPG) axis. *Sci Rep*. 2017;7:45125.
28. Aubin-Horth N, Landry CR, Letcher BH, Hofmann HA. Alternative life histories shape brain gene expression profiles in males of the same population. *Proc Biol Sci*. 2005;272:1655-1662.
29. Renn SCP, Aubin-Horth N, Hofmann HA. Fish and chips: functional genomics of social plasticity in an African cichlid fish. *J Exp Biol*. 2008; 211:3041-3056.
30. Heyne HO, Lautenschlager S, Nelson R, et al. Genetic influences on brain gene expression in rats selected for tameness and aggression. *Genetics*. 2014;198:1277-1290.
31. Sen Sarma M, Whitfield CW, Robinson GE. Species differences in brain gene expression profiles associated with adult behavioral maturation in honey bees. *BMC Genomics*. 2007;8:202.
32. Toth AL, Varala K, Henshaw MT, Rodriguez-Zas SL, Hudson ME, Robinson GE. Brain transcriptomic analysis in paper wasps identifies genes associated with behaviour across social insect lineages. *Proc Biol Sci*. 2010;277:2139-2148.
33. Harris RM, Hofmann HA. Neurogenomics of behavioral plasticity. *Adv Exp Med Biol*. 2014;781:149-168.
34. Oldham MC, Horvath S, Geschwind DH. Conservation and evolution of gene coexpression networks in human and chimpanzee brains. *Proc Natl Acad Sci U S A*. 2006;103:17973-17978.
35. Drnevich J, Replogle KL, Lovell P, et al. Impact of experience-dependent and -independent factors on gene expression in songbird brain. *Proc Natl Acad Sci U S A*. 2012;109(Suppl 2):17245-17252.
36. Sanogo YO, Band M, Blatti C, Sinha S, Bell AM. Transcriptional regulation of brain gene expression in response to a territorial intrusion. *Proc Biol Sci*. 2012;279:4929-4938.
37. Derycke S, Kéver L, Herten K, et al. Neurogenomic profiling reveals distinct gene expression profiles between brain parts that are consistent in ophthalmotilapia cichlids. *Front Neurosci*. 2018;12:136.
38. Xu X, Coats JK, Yang CF, et al. Modular genetic control of sexually dimorphic behaviors. *Cell*. 2012;148:596-607.
39. Peterson MP, Rosvall KA, Choi JH, et al. Testosterone affects neural gene expression differently in male and female juncos: a role for hormones in mediating sexual dimorphism and conflict. *PLoS One*. 2013;8: e61784.
40. Zinzow-Kramer WM, Horton BM, McKee CD, et al. Genes located in a chromosomal inversion are correlated with territorial song in white-throated sparrows. *Genes Brain Behav*. 2015;14:641-654.
41. Rosvall KA, Bergeon Burns CM, Barske J, et al. Neural sensitivity to sex steroids predicts individual differences in aggression: implications for behavioural evolution. *Proc Biol Sci*. 2012;279:3547-3555.
42. Horton BM, Hudson WH, Ortlund EA, et al. Estrogen receptor α polymorphism in a species with alternative behavioral phenotypes. *Proc Natl Acad Sci U S A*. 2014;111:1443-1448.
43. Ryder TB, Parker PG, Blake JG, Loiselle BA. It takes two to tango: reproductive skew and social correlates of male mating success in a lek-breeding bird. *Proc Biol Sci*. 2009;276:2377-2384.
44. Ryder TB, McDonald DB, Blake JG, Parker PG, Loiselle BA. Social networks in the lek-mating wire-tailed manakin (*Pipra filicauda*). *Proc Biol Sci*. 2008;275:1367-1374.
45. Ryder TB, Horton BM, Moore IT. Understanding testosterone variation in a tropical lek-breeding bird. *Biol Lett*. 2011;7:506-509.
46. Martínez-García F, Novejarque A, Lanuza E. Evolution of the amygdala in vertebrates. In: Kaas J, ed. *Evolution of Nervous System, Nonmammalian Vertebrates*. Vol 2. Amsterdam, Netherlands: Elsevier, Academic Press; 2006:258-334.
47. Martínez-García F, Martínez-Marcos A, Lanuza E. The pallial amygdala of amniote vertebrates: evolution of the concept, evolution of the structure. *Brain Res Bull*. 2002;57:463-469.
48. Kingsbury MA, Kelly AM, Schrock SE, Goodson JL. Mammal-like organization of the avian midbrain central gray and a reappraisal of the intercollicular nucleus. *PLoS One*. 2011;6:e20720.
49. Fusani L, Donaldson Z, London SE, Fuxjager MJ, Schlinger BA. Expression of androgen receptor in the brain of a sub-oscine bird with an elaborate courtship display. *Neurosci Lett*. 2014;578:61-65.
50. Stokes TM, Leonard CM, Nottebohm F. The telencephalon, diencephalon, and mesencephalon of the canary, *Serinus canaria*, in stereotaxic coordinates. *J Comp Neurol*. 1974;156:337-374.
51. Kelly AM, Kingsbury MA, Hoffbuhr K, et al. Vasotocin neurons and septal V1a-like receptors potently modulate songbird flocking and responses to novelty. *Horm Behav*. 2011;60:12-21.
52. Goodson JL, Evans AK, Lindberg L. Chemoarchitectonic subdivisions of the songbird septum and a comparative overview of septum chemical anatomy in jawed vertebrates. *J Comp Neurol*. 2004;473: 293-314.
53. Wild JM. The ventromedial hypothalamic nucleus in the zebra finch (*Taeniopygia guttata*): afferent and efferent projections in relation to the control of reproductive behavior. *J Comp Neurol*. 2017;525:2657-2676.
54. Riters LV, Ball GF. Lesions to the medial preoptic area affect singing in the male European starling (*Sturnus vulgaris*). *Horm Behav*. 1999;36: 276-286.
55. Krueger F. Trim Galore! A wrapper tool around Cutadapt and FastQC to consistently apply quality and adapter trimming to FastQ files. 2015. http://www.bioinformatics.babraham.ac.uk/projects/trim_galore/
56. Kim D, Langmead B, Salzberg SL. HISAT: a fast spliced aligner with low memory requirements. *Nat Methods*. 2015;12:357-360.
57. Ohlson JI, Fjeldså J, Ericson PGP. Molecular phylogeny of the manakins (Aves: Passeriformes: Pipridae), with a new classification and the description of a new genus. *Mol Phylogenet Evol*. 2013;69:796-804.
58. Anders S, Pyl PT, Huber W. HTSeq–a Python framework to work with high-throughput sequencing data. *Bioinforma Oxf Engl*. 2015;31: 166-169.
59. Anders S, Huber W. Differential expression analysis for sequence count data. *Genome Biol*. 2010;11:R106.
60. Love MI, Huber W, Anders S. Moderated estimation of fold change and dispersion for RNA-seq data with DESeq2. *Genome Biol*. 2014; 15:550.
61. Marini F. *pcaExplorer–Interactive Exploration of Principal Components of Samples and Genes in RNA-seq Data*; 2018.
62. Langfelder P, Horvath S. WGCNA: an R package for weighted correlation network analysis. *BMC Bioinformatics*. 2008;9:559.
63. Langfelder P, Horvath S. Fast R functions for robust correlations and hierarchical clustering. *J Stat Softw*. 2012;46:i11.
64. Eden E, Navon R, Steinfeld I, Lipson D, Yakhini Z. GOrilla: a tool for discovery and visualization of enriched GO terms in ranked gene lists. *BMC Bioinformatics*. 2009;10:48.
65. R Core Team. *R: A Language and Environment for Statistical Computing*. Vienna, Austria: R Foundation for Statistical Computing; 2013.
66. Csardi G, Nepusz T. The igraph software package for complex network research. *Inter Journal Complex Syst*. 2006;1695:1-9.
67. Gu Z, Rifkin SA, White KP, Li W-H. Duplicate genes increase gene expression diversity within and between species. *Nat Genet*. 2004;36: 577-579.
68. Li W-H, Yang J, Gu X. Expression divergence between duplicate genes. *Trends Genet TIG*. 2005;21:602-607.
69. Thornton JW. Evolution of vertebrate steroid receptors from an ancestral estrogen receptor by ligand exploitation and serial genome expansions. *Proc Natl Acad Sci U S A*. 2001;98:5671-5676.

70. Escriva H, Bertrand S, Germain P, et al. Neofunctionalization in vertebrates: the example of retinoic acid receptors. *PLoS Genet*. 2006;2:e102.
71. Baxter MG, Murray EA. The amygdala and reward. *Nat Rev Neurosci*. 2002;3:563-573.
72. Seigneur E, Südhof TC. Genetic ablation of all cerebellins reveals synapse organizer functions in multiple regions throughout the brain. *J Neurosci*. 2018;38:4774-4790.
73. Gundlach AL, Burazin TC, Larm JA. Distribution, regulation and role of hypothalamic galanin systems: renewed interest in a pleiotropic peptide family. *Clin Exp Pharmacol Physiol*. 2001;28:100-105.
74. Wodowska J, Ciosek J. Galanin and galanin-like peptide modulate vasopressin and oxytocin release in vitro: the role of galanin receptors. *Neuropeptides*. 2014;48:387-397.
75. Robinson J, Brewer A. Galanin: A potential role in mesolimbic dopamine-mediated instrumental behavior. *Neurosci Biobehav Rev*. 2008;32:1485-1493.
76. Wang W, Lufkin T. The murine Otp homeobox gene plays an essential role in the specification of neuronal cell lineages in the developing hypothalamus. *Dev Biol*. 2000;227:432-449.
77. Wang L et al. Differentiation of hypothalamic-like neurons from human pluripotent stem cells. *J Clin Invest*. 2105;125:796-808.
78. Yamamoto K, Mirabeau O, Bureau C, et al. Evolution of dopamine receptor genes of the D1 class in vertebrates. *Mol Biol Evol*. 2013;30:833-843.

SUPPORTING INFORMATION

Additional supporting information may be found online in the Supporting Information section at the end of this article.

How to cite this article: Horton BM, Ryder TB, Moore IT, Balakrishnan CN. Gene expression in the social behavior network of the wire-tailed manakin (*Pipra filicauda*) brain. *Genes, Brain and Behavior*. 2020;19:e12560. https://doi.org/10.1111/gbb.12560